ON THE INFLUENCE OF SPATIAL RESOLUTION IN SOIL SURFACE ROUGHNESS CHARACTERIZATION USING TLS AND SFM TECHNIQUES

Alex Martinez-Agirre, Jesús Álvarez-Mozos and Rafael Giménez

Public University of Navarre, Department of Projects and Rural Engineering, Campus Arrosadia (31006), Pamplona (Spain)

ABSTRACT

Soil surface roughness strongly affects the scattering of microwaves and determines the backscattering coefficient observed by SAR (Synthetic Aperture Radar) sensors. The aim of this study is to analyze the influence of the spatial resolution of Terrestrial Laser Scanner (TLS) and Structure from Motion (SfM) techniques to parameterize surface roughness over agricultural soils. Three experimental plots (5 x 5 meters) representing different roughness conditions were measured by TLS and SfM techniques. Roughness parameters (*s* and *l*) were calculated from profiles obtained at different spatial resolutions in parallel and in perpendicular to the tillage direction on each plot. The results showed minor differences in the parameters values between both techniques and, in general, a decreasing trend and an increasing trend for lower spatial resolutions for parameter *s* and *l*, respectively.

***Index Terms*—** Surface roughness, measurement techniques, TLS, SfM, spatial resolution

1. INTRODUCTION

Soil surface roughness can be defined as the variations in soil surface elevation from a reference surface [1]. In agricultural areas surface roughness is directly related to tillage, whose action strongly affects the key physical properties of soil and determines the occurrence and fate of several processes (e.g. surface storage, infiltration, etc.). At the same time, surface roughness strongly affects the scattering of microwaves at the soil surface and determines the backscattering coefficient observed by radar sensors.

The complexity of roughness reflects the wide range of surface measurement techniques used for its parameterization [2]. The resolution, extent and availability of surface elevation datasets have been spectacularly improved over the last years [3]. Nowadays, the most commonly used techniques for surface roughness measurements are laser scanners and image based 3D reconstruction technologies [4], [5]. Specifically, Terrestrial Laser Scanner (TLS) technique presents accuracies of 0.1-0.5 mm for vertical measurements and 0.1-2 mm for horizontal ones [6]. On the other hand, image based 3D reconstruction technologies can be divided into traditional stereo-photogrammetry and Structure from Motion (SfM) photogrammetry [5]. In the last years, the interest of scientist in this technology as a surface reconstruction tool has expanded since the development of readily available SfM software (e.g. [5], [7]).

In this work, TLS and SfM measurement techniques were used for the characterization of surface roughness in agricultural soils, and the influence of the spatial resolution considered to obtain roughness parameters was addressed.

2. MATERIALS AND METHODS

2.1. Test site

The study was carried out in the experimental fields at the School of Agricultural Engineers of the Public University of Navarre in Pamplona (Navarre, Spain) (42.79º N, 1.63º W). The soils have a silty-clay-loam texture (13.7% sand, 48.3% silt and 38% clay). Three experimental plots (5x5 meters) were created using different tillage implements for representing different surface roughness conditions. Plot 1 corresponds to low roughness conditions (Moldboard Plough + Harrowed Compacted) (HC), Plot 2 to medium roughness (Chisel) (CH), and Plot 3 to high roughness (Moldboard Plough) (MP).

2.2. Measuring techniques

Surface roughness data collection was performed using Terrestrial Laser Scanner (TLS) and Structure from Motion (SfM) techniques.

The TLS instrument used in this analysis was the FARO Focus 3D (Fig. 1). Four scans were obtained per plot (i.e., one from each side) from a tripod ~1.75 m high. Five reference spheres were deployed around the plot for scans co-registration. This instrument has a specific ranging precision of 0.3 mm (90% reflectivity) and a beam divergence of 0.16 mrad (0.009º) with a diameter of 3.8 mm. The scan vertical and horizontal resolution was set in 0.0018º (20480 3D pixels in 360º), resulting in a maximum sampling interval of 1.8 mm.

Fig. 1. FARO Focus 3D (left) and the scanning setup (right).

SfM technology is based on a set of overlapping photographs from different points of view. In this study, 24 photos of 20 megapixels were acquired for each plot using a Canon EOS 5D Mark II camera with a 21 mm objective (Fig. 2). Photos were homogeneously distributed and acquired from a height of ~8 meters (using a lifting platform) capturing the entire experimental plot from each photo.

Fig. 2. Canon EOS 5D Mark II (left) and the lifting platform (right).

2.3. Data pre-processing

TLS scans were filtered, co-registered and merged into a single point cloud. The co-registration of individual scans was done using the ICP (iterative closest point) algorithm implemented in the OPALS software [8]. The standard deviation was about 1.1 mm for HC and CH plots and 2.5 mm for MP. After merging the individual co-registered scans, ~30 million point cloud was obtained for each plot (Table 1).

For SfM data processing, eight control points were used for referencing, obtaining a mean error about 1.1 mm for HC, 1.6 mm for CH and 1.9 mm for MP. The point cloud was generated in “ultra-high quality” mode using the software Agisoft PhotoScan, with an average point spacing of ~1.7 mm corresponding to a minimum of 10 million points for each plot (Table 1).

Table 1. Details of the point clouds obtained after processing

Plot	Measurement technique	Nº of points
HC	Terrestrial Laser Scanner (TLS)	31.964.773
HC	Structure from Motion (SfM)	11.548.505
CH	Terrestrial Laser Scanner (TLS)	26.513.592
CH	Structure from Motion (SfM)	13.507.994
MP	Terrestrial Laser Scanner (TLS)	30.447.219
MP	Structure from Motion (SfM)	17.303.166

2.4. Data analysis

The analysis presented here focused on the influence of the spatial resolution of the elevation data for surface roughness characterization in agricultural soils. First, the point clouds obtained with TLS and SfM were co-registered using again IPC algorithm. The error (standard deviation of the plane-to-plane residuals) was less than 2 mm for the three plots. Then, 4 m long profiles were extracted (four in parallel and four in perpendicular to tillage direction for each plot) considering all the points of the cloud closer than a threshold (depending on the resolution). Then, these points were (1) filtered to avoid occlusions, (2) binned at different intervals (2.5, 5, 10, 20 and 40 mm) and (3) interpolated to avoid empty data. Finally, roughness parameters of each profile extracted at different resolutions (intervals) were calculated and analyzed.

2.4.1. Roughness parameters

The two mostly used roughness parameters for radar remote sensing applications were analyzed, i.e. the standard deviation of heights (*s*) and the correlation length (*l*). The standard deviation of heights (*s*) is a descriptor of the vertical roughness component:

$$s = \sqrt{\frac{\sum_{i=1}^{N}(z_i{}^2 - \bar{z}^2)}{N-1}} \qquad (1)$$

where N is the number of the records registered in the profile, z_i is the height corresponding to record i, and $\bar{z}$ is the mean height of all the records. The correlation length (*l*) represents the horizontal component of roughness and is defined as the distance at which the heights of two points on the surface are considered independent. The correlation length is obtained from the autocorrelation function [1]:

$$\rho(h) = \frac{\sum_{i=1}^{N(h)} z_i z_{i+h}}{\sum_{i=1}^{N} z_i{}^2} \qquad (2)$$

where $\rho(h)$ is the autocorrelation function, representing the correlation existing between height of the point i (z_i) and that of another point located at a lag distance h from it (z_{i+h}), and $N(h)$ is the number of pairs considered in each lag h. The correlation length (*l*) is then defined as the distance at which the heights of two points on the profile are considered independent; i.e., $\rho(h)$ is equal to $1/e$, so that $\rho(l) = 1/e$.

3. RESULTS AND DISCUSSION

A first visual exploration of the same profile at different resolutions obtained with both TLS and SfM techniques reveals interesting details (Fig. 3).

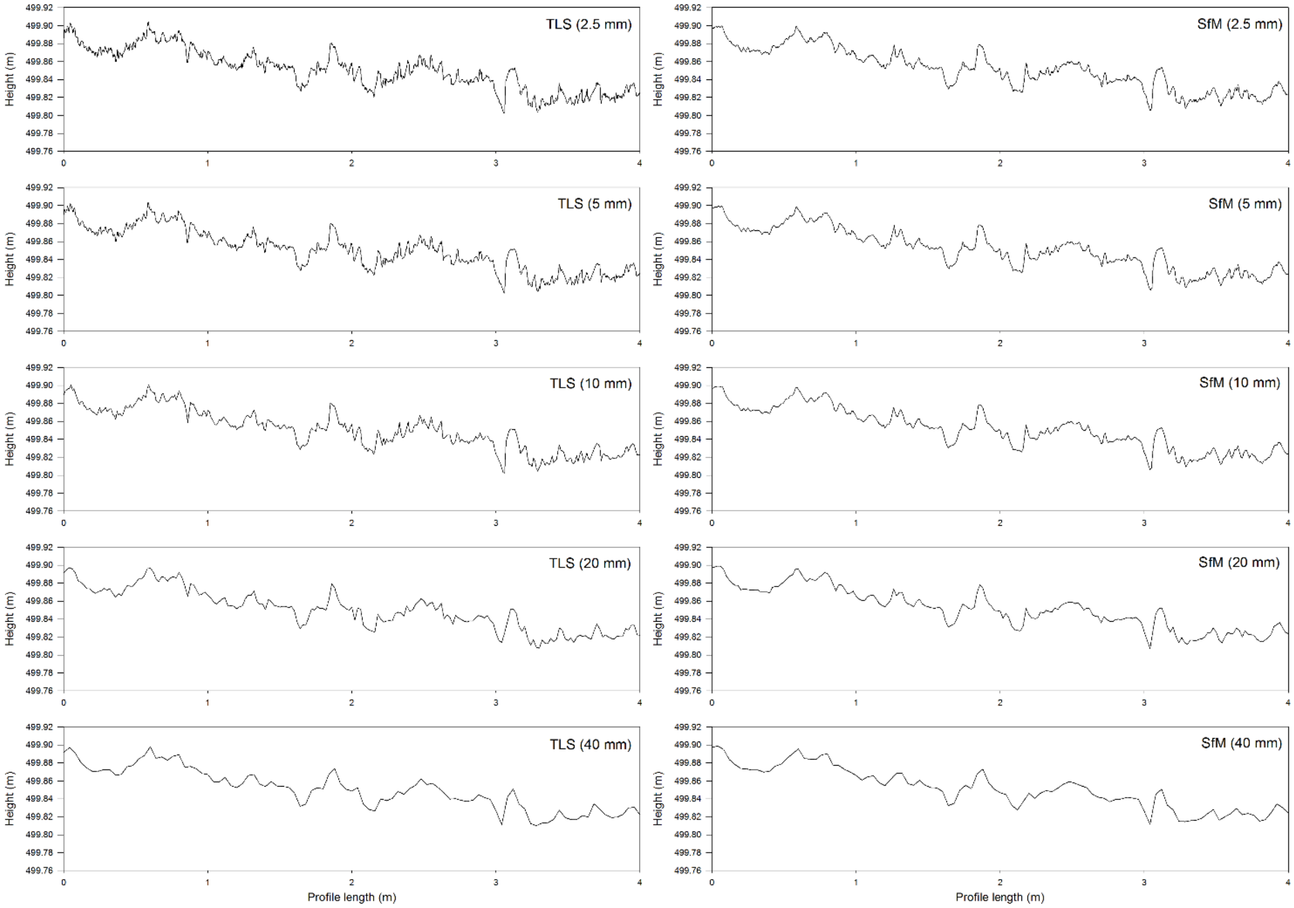

Fig. 3. Example profile at different resolutions obtained with TLS (left column) and SfM (right column) measurement techniques.

Although, profiles at different resolutions showed a similar behavior, some differences were noticed. At high resolutions (intervals < 10 mm), profiles obtained with TLS technique seemed to be more sensitive to high frequency (small-scale) roughness components than SfM ones. However, at medium and low resolutions (intervals > 10 mm), little differences were observed between both techniques.

The mean values of *s* and *l* parameters for each experimental plot in parallel (P) and in perpendicular (T) to the tillage direction were obtained (Table 2 and 3).

Table 2. Mean values of parameter *s* (cm) depending on the resolution.

	2.5 mm	**5 mm**	**10 mm**	**20 mm**	**40 mm**
CH (P) (TLS)	1.346	1.349	1.329	1.295	1.221
CH (P) (SfM)	1.246	1.245	1.236	1.211	1.123
CH (T) (TLS)	1.830	1.827	1.821	1.809	1.750
CH (T) (SfM)	1.759	1.758	1.752	1.746	1.696
HC (P) (TLS)	1.093	1.090	1.075	1.057	1.007
HC (P) (SfM)	0.996	0.999	0.992	0.993	0.958
HC (T) (TLS)	1.418	1.415	1.408	1.399	1.379
HC (T) (SfM)	1.400	1.400	1.398	1.393	1.383
MP (P) (TLS)	3.588	3.601	3.597	3.517	3.430
MP (P) (SfM)	3.650	3.642	3.641	3.603	3.509
MP (T) (TLS)	4.369	4.364	4.369	4.322	4.175
MP (T) (SfM)	4.369	4.366	4.357	4.340	4.215

Table 3. Mean values of parameter *l* (cm) depending on the resolution.

	2.5 mm	**5 mm**	**10 mm**	**20 mm**	**40 mm**
CH (P) (TLS)	7.912	8.019	8.023	11.515	13.278
CH (P) (SfM)	6.132	6.803	8.283	10.389	14.773
CH (T) (TLS)	9.891	9.880	9.865	10.031	28.014
CH (T) (SfM)	10.041	10.049	10.081	10.953	26.188
HC (P) (TLS)	21.621	21.525	23.482	24.836	22.040
HC (P) (SfM)	29.058	29.127	29.294	30.570	30.962
HC (T) (TLS)	27.274	27.335	27.470	28.365	30.171
HC (T) (SfM)	28.184	28.246	28.256	28.584	29.090
MP (P) (TLS)	11.946	12.015	12.018	12.596	14.277
MP (P) (SfM)	10.311	10.333	10.363	10.945	14.346
MP (T) (TLS)	13.423	13.461	13.430	13.833	19.783
MP (T) (SfM)	14.365	14.365	14.412	14.542	20.159

As expected, *s* parameter values were low for HC plot, intermediate for CH plot and extremely high for MP plot, and also showed higher values in perpendicular than in parallel to the tillage direction. The mean values of parameter *s* showed slightly higher values for TLS technique (with the exception of MP plot in parallel). However, mean values of parameter *l* showed higher values for SfM (with the exception of CH plot in parallel at higher resolutions and MP plot in parallel).

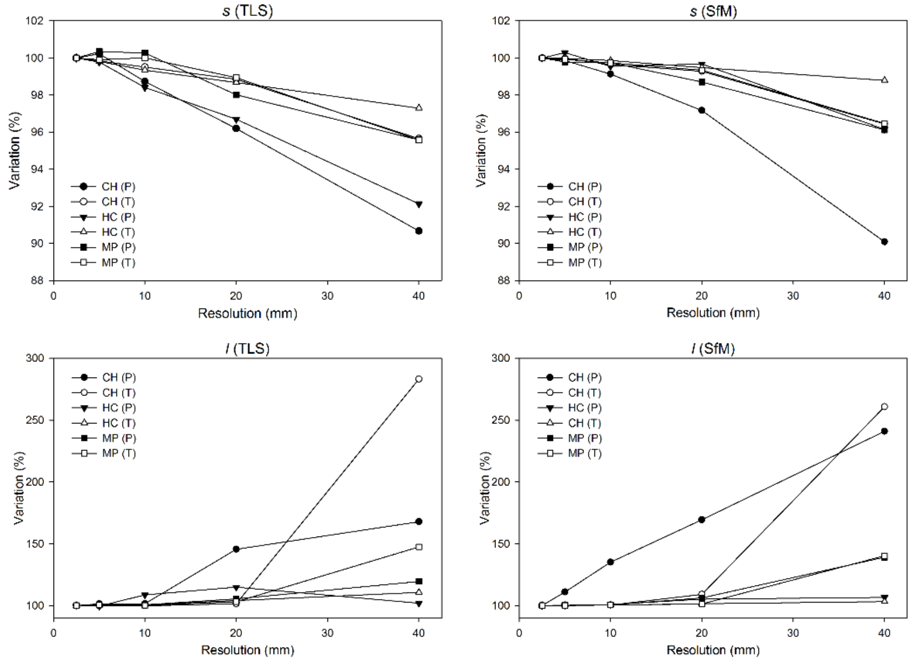

Fig. 4. Variation of the mean values of *s* and *l* parameters depending on the resolution.

In relative terms (Fig. 4) TLS and SfM techniques showed the highest variations (positive or negative) when the lowest resolutions (highest intervals) chosen. However, *s* variation rate was normally below %5 (except a maximum value of %10 for HC), whereas *l* variation rate was much larger. Particularly, for parameter *s* the smoothest field (HC) measured in parallel to tillage showed the highest relative variation, whereas for parameter *l* the intermediate CH field had the highest variation in both techniques.

4. CONCLUSIONS

The results showed a reasonable agreement between the elevation profiles obtained with TLS and SfM. However, at high spatial resolutions profiles obtained with TLS seemed to be more sensitive to high frequency roughness components. In general, mean values of parameter *s* showed slightly higher values for TLS, while mean values of parameter *l* showed higher values for SfM. In relative terms, both techniques showed the highest variations when the lowest resolution was chosen. However, *s* sensitivity to spatial resolution was rather low, whereas *l* was much more sensitive.

5. ACKNOWLEDGEMENTS

This work was partly funded by project CGL2016-75217-R (MINECO/FEDER, EU).

6. REFERENCES

[1] F.T. Ulaby, R.K. Moore, A.K. Fung, *Microwave remote sensing: active and passive. Volume II: Radar remote sensing and surface scattering and emission theory*, Addison-Wesley, Reading, MA, USA, 1982.

[2] M.W. Smith, “Roughness in the Earth Sciences”, *Earth Sci. Rev.*, *136*, pp. 202-225, 2014.

[3] D. Vericat, M.W. Smith, J. Brasington, “Patterns of topographic change in sub-humid badlands determined by high resolution multi-temporal topographic surveys”, *Catena*, 120, pp. 164-176, 2014.

[4] R.J. Barneveld, M. Seeger, I. Maalen-Johansen, “Assessment of terrestrial laser scanning technology for obtaining high-resolution DEMs of soils”, *Earth Surf. Proc. Land.*, 38 (1), pp. 90-94, 2013.

[5] Nouwakpo, S.K., Weltz, M.A., McGwire, K., 2016. Assessing the performance of structure-from-motion photogrammetry and terrestrial LiDAR for reconstructing soil surface microtopography of naturally vegetated plots. Earth Surf. Proc. Land. 41 (3), 308-322.

[6] M.A. Aguilar, F.J. Aguilar, J. Negreiros, “Off-the-shelf laser scanning and close-range digital photogrammetry for measuring agricultural soils microrelief”, *Biosyst. Eng.*, 103 (4), pp. 504-517, 2009.

[7] M.W. Smith, D. Vericat, “From experimental plots to experimental landscapes: topography, erosion and deposition in sub-humid badlands from Structure-from-Motion photogrammetry”, *Earth Surf. Process. Landforms*, 40 (2), pp. 1656-1671, 2015.

[8] N. Pfeifer, G. Mandlburger, J. Otepka, W. Karel, “OPALS - A framework for Airborne Laser Scanning data analysis”, *Comput. Environ. Urban Syst.*, 45, pp. 125-136, 2014.